



Radiometric mapping and radiation dose assessments in sediments from Şavşat Black Lake, Turkey

Serdar Dizman¹ · Tolga Akdemir² · Cafer Mert Yeşilkanat³ · Vagif Nevruzoglu⁴ · Esra Bal⁵ · Recep Keser⁶

Received: 6 December 2021 / Accepted: 19 April 2022 / Published online: 11 May 2022
© Akadémiai Kiadó, Budapest, Hungary 2022

Abstract

In this study, natural and artificial radioactivity concentrations in sediment samples taken from Şavşat Black Lake located on the Nature Park in Artvin were determined using a high purity germanium detector. It was determined that ²³⁸U, ²³²Th, ⁴⁰K and ¹³⁷Cs radioisotope concentrations in the sediment samples varied between 8.15 and 32.67, 5.83 and 33.08, 185.88 and 589.30, and 0.86 and 438.04 Bq kg⁻¹, respectively. In order to evaluate the radiological hazards, some radiological parameters were calculated and compared with the values recommended by international organizations. The results showed that the sediments in the study area will not pose any health risk for the visitors of Şavşat Black Lake.

Keywords Radionuclides · Absorbed dose rate · Radiation hazard · Radiological map · ¹³⁷Cs

Introduction

Long-half-life radiolucides found naturally in soils, rocks, water, sediments and similar materials in nature form a background radiation that is considered normal and inevitable in the lived environment. People are constantly exposed to background radiation created by these sources in their natural environment.

Natural resources have a very important place in radiation dose evaluations. It is because people receive certain doses of radiation from natural sources throughout their lives [1, 2]. The radiation received over the years can cause certain

damage to the body after a while, and even this damage can result in death. The main purpose of environmental radiation measurements is to determine the dose of radiation, as well as the type of radiation that people receive from environmental sources, and to evaluate the risk it will create. This requires determining the concentrations of radionuclides that are natural sources of radiation in the surrounding environment, as well as the effect of radiation on biological systems, particularly humans [2]. Additionally, a relationship should be established between radionuclides in the surrounding environment and the radiation dose received by people from these sources. Only after conducting such research it can be determined whether a region is radiation-safe for a healthy life [3, 4]. To estimate the natural and artificial radiation dose of different environments in the world, previous research has been conducted on natural radioactivity levels in the sediments of rivers, lakes and coasts [5–12]. However, research concerning the natural and artificial radioactivity levels of lake bottom sediments is limited. In the studies carried out by Kobya et al. and Yeşilkanat et al. on the distribution of environmental radiation, it was mapped that the distribution of absorbed gamma dose rate level was at high levels for the study area examined in this study. It is important to examine this situation, which is one of the main motivation sources of this research, and to evaluate it especially in terms of the health of people who come to the region for tourism purposes and who live in the region. In addition to these, since it is a natural park and under protection by the

✉ Serdar Dizman
serdar.dizman@erdogan.edu.tr

¹ Department of Physics, Faculty of Arts and Science, Recep Tayyip Erdogan University, 53100 Rize, Turkey

² Vocational School of Technical Sciences, Recep Tayyip Erdogan University, 53100 Rize, Turkey

³ Science Teaching Department, Artvin Çoruh University, 08100 Artvin, Turkey

⁴ Department of Energy Systems Engineering, Faculty of Engineering and Architecture, Recep Tayyip Erdogan University, 53100 Rize, Turkey

⁵ High Chemist and Occupational Safety Specialist, Rize Municipality, 53100 Rize, Turkey

⁶ Department of Basic Sciences, Faculty of Engineering, Samsun University, 55100 Samsun, Turkey

state, the study area is not polluted by secondary pollutants of human or industrial origin. This provides important information in terms of revealing the levels of both natural background radiation and artificial radiation in a local area [5, 13]. In addition, the detection of ^{137}Cs radioisotope in the regions around the lake in previous studies, shows that the effects of the reactor accident at the Chernobyl Nuclear Power Plant close to Turkey, as well as the effects of nuclear tests are still continue [5, 10, 13–15].

This study aims to determine the natural and artificial radioactivity levels in the bottom sediment samples of Şavşat Black Lake located in Karagöl-Sahara National Park in Artvin province and compare the obtained values with the permissible limit values accepted by United Nations Scientific Committee on the Effects of Atomic Radiation (UNSCEAR) and International Commission on Radiological Protection (ICRP). In addition, it aims to calculate the radiological hazard parameters (radium equivalent activity, external hazard index, absorbed dose rate, annual effective dose equivalent, and cancer risk ratio), to evaluate the studied area in terms of radiological risk and to determine whether there is any radiological risk for people visiting Black Lake.

Materials and methods

Study area

The study area is Şavşat Black Lake, located 25 km north of Artvin's Şavşat district and at an altitude of 1650 m (Fig. 1). Black Lake is a landslide lake located in the Karagöl-Sahara National Park, which was declared as a National Park in 1994, at the coordinates 41.309 N–41.307 N and 42.482 E–42.486 E [16]. The area of Şavşat Black Lake is approximately 50,000 m² and its deepest point is 33 m. The region is generally composed of palaeogene and neogene lands. Most of the rocks in the region are of sedimentary origin. Black Lake and its surroundings exhibit a unique topographic character, with valleys dividing them in half. These cleavages have caused landslides and mass movements to be active in the region. The area surrounding the lake is densely forested, primarily with spruce and pine. The climate of the Karagöl is generally cool and rainy in summer and cold and snowy in winter. According to the climate data obtained from the Şavşat meteorology station, the annual average temperature of Karagöl and its surroundings is 9.8 °C. The lowest average temperature value was measured as –1.9 °C in January and the highest average temperature value was 20.6 °C in August. The average annual precipitation in the region is 737.9 mm. The least precipitation fall in August, the most precipitation fall in June [17]. The site has an important potential for various tourism activities, especially eco-tourism. Black Lake and its surroundings are also utilized as

a recreation area. It is possible to set up tents and camp around the lake. Located in the National Park, Şavşat Black Lake was visited by 32,276 people in 2017 and by a total of 146,896 people between 2010 and 2017 [16, 18].

Sample collection and preparation for analysis

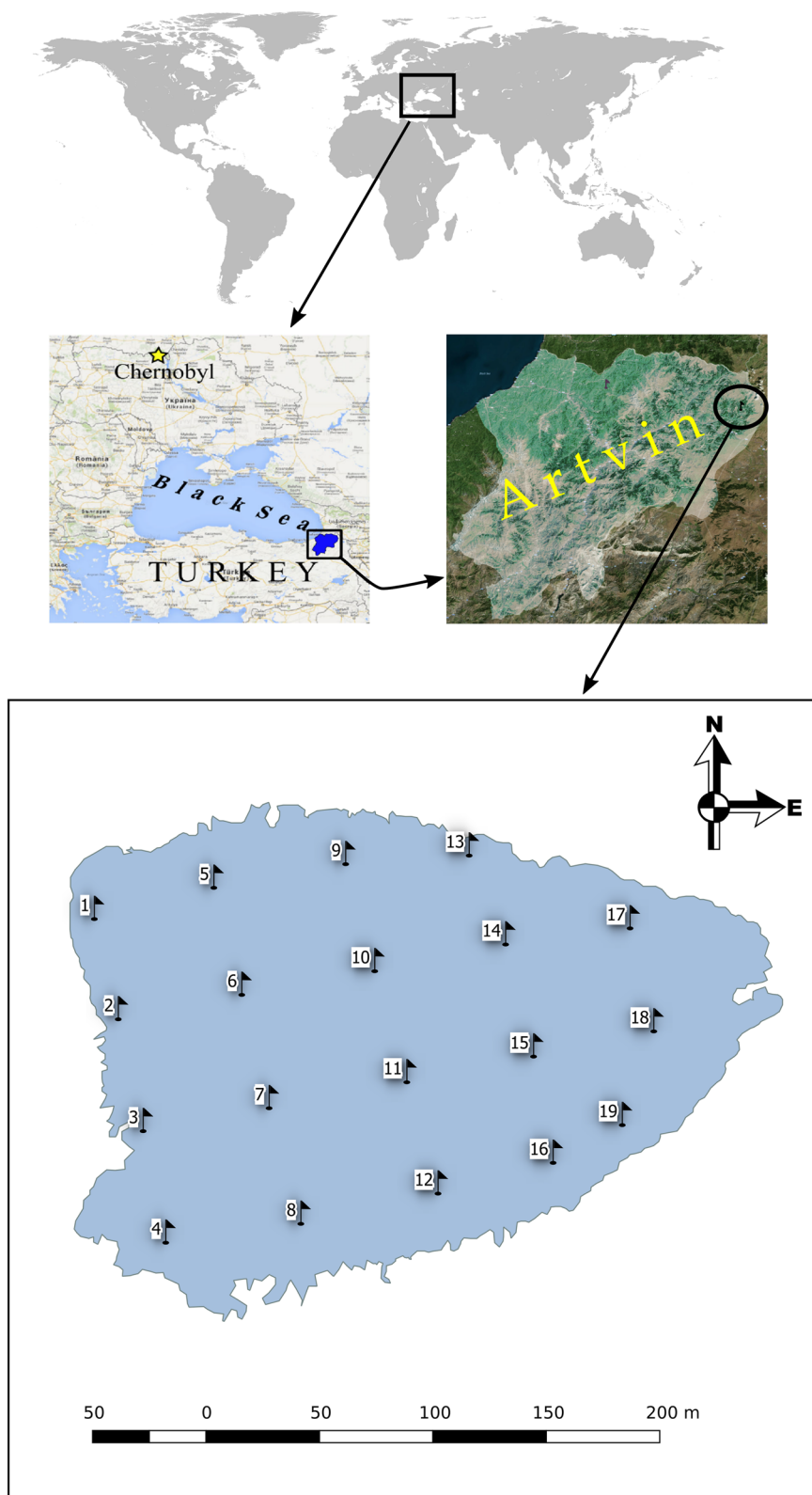
In July 2019, 19 sediment samples were collected, one sediment sample (approximately 2 kg) from each of the small equal areas of Black Lake was determined using the grilling method (Fig. 1). Sediment samples were collected using Ekman-Birge grab equipment (Hydro Bios Apparatebau GmbH, Kiel-Altenholztip, Germany). Samples were collected by scuba diving in places where sediment samples could not be collected using Ekman-Birge grab equipment. Boat was used during the collection of samples. In addition, the coordinates of each sampling point were recorded using a GPS device (Magellan Explorist 510). The collected samples were then transported to the laboratory.

The samples were first separated from foreign materials such as stones, wood chips and plant roots and allowed to dry at room temperature for at least 24 h. Then the samples were dried for 24 h in a drying oven set at 105 °C. The dried samples were then ground in agate mortar and passed through a 300 (45 µm) mesh sieve to reduce the particle size effect. The sieved samples were placed in airtight polyethylene sample cups and their masses were determined. Finally, the prepared samples were kept for 1 month to reach the radioactive equilibrium.

Determination of radioactivity

Activity concentration measurements of ^{238}U , ^{232}Th , ^{40}K and ^{137}Cs radioisotopes were carried out using ORTEC brand (Model: GEM55P4-95) High Purity Germanium Detector (HPGe), which has a separation power (resolution) of 1.9 keV at 1332.5 keV and relative efficiency of 55%. Separation power can literally be referred to as the resolution of a detector. High resolution enables the separation of two gamma lines which are close to each other thereby eliminating spectral interferences. The energy resolution of a detector is typically discussed in terms of the full width half maximum (FWHM) of the peak in related gamma-ray energy. The gamma spectrometer system consists of a detector, a preamplifier, a spectroscopy amplifier, an ADC system that converts analog counts into electronic signals and a multichannel analyzer (MCA). The detector's sample chamber is shielded with a 10 cm lead block against background radiation from construction materials and cosmic rays. The prepared samples were counted for 50,000 s in the detector and the image of one of the obtained spectra is presented in Fig. 2. Gamma Vision, a data analysis program, was used to evaluate the

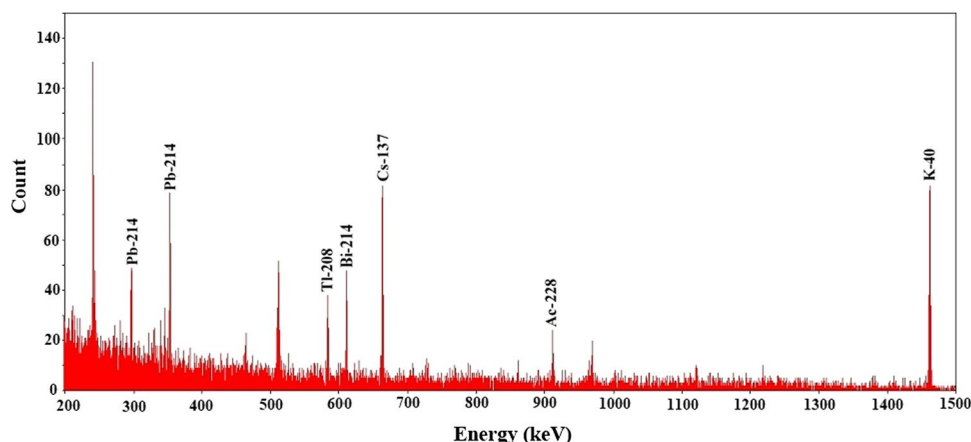
Fig. 1 The study area and sampling points



spectra obtained from counting. The area of the peaks at the energies of 295.2 keV and 352 keV for ^{214}Pb , and 609.4 keV for ^{214}Bi were used for the determination of the

activity concentration of the ^{238}U radioisotope, while the areas of the peaks at 583.1 keV of ^{208}Tl and 911.1 keV of ^{228}Ac were used for the determination of the activity

Fig. 2 A typical spectrum image obtained from measuring samples at the detector



concentration of the ^{232}Th radioisotope. The areas of the peaks with energies of 1460.8 keV and 661.6 keV, respectively, were used to calculate the activity concentrations of the ^{40}K and ^{137}Cs radioisotopes. The radioactivity concentrations of the sediment samples after determining the peak areas at these energies were calculated using Eq. 1.

$$A(\text{Bqkg}^{-1}) = \frac{N}{\varepsilon \cdot I_{\gamma} \cdot t \cdot m} \quad (1)$$

N is the net area at the energy of interest, ε is the efficiency at the gamma energy of interest, I_{γ} is the abundance of the gamma ray at the energy of interest, t is the count time (s) and m is the sample mass (kg).

Detector efficiency should be determined for each observed peak in the spectrum to determine the actual value of the gamma counts that the detector has detected [19]. For this, the ^{152}Eu standard source was placed in front of the detector and counted for 10 min and then the count rate values of the formed spectra were obtained. Using these count rate values, detector efficiencies at energies of interest were calculated using Eq. 2.

$$\varepsilon = \frac{N}{A \cdot I_{\gamma}} \quad (2)$$

ε is the efficiency at the gamma energy of interest, N is the total count rate at the energy of interest (counts/time), A is the current activity (Bq) of the standard source used for the efficiency calibration and I_{γ} is the abundance of gamma rays at the energy of interest.

The minimum detectable activity (MDA) values for the respective radioisotopes in the germanium detector were calculated using Eq. 3 [20].

$$\text{MDA}(\text{Bqkg}^{-1}) = \frac{4,66\sqrt{B}}{\varepsilon \cdot I_{\gamma} \cdot t \cdot m} \quad (3)$$

B is the area of the background count at the energy of interest, ε is the efficiency at the gamma energy of interest, I_{γ} is the abundance of the gamma-ray at the energy of interest, t is the count time (s) and m is the sample mass (kg).

The accuracy of the measurement system was checked using the certified soil reference sample (IAEA-375). Accuracy expressed as a recovery of soil reference sample was obtained in the range of 94–98% for the measured radionuclides in this study.

Calculation of radiological effects

Radium equivalent activity

The distribution of ^{238}U , ^{232}Th and ^{40}K in the environment is different from each other. To standardize the exposure to radiation from these specific activities at different amounts, the radium equivalent activity (Ra_{eq}) is defined and this value is calculated by Eq. 4 [21].

$$Ra_{\text{eq}}(\text{Bq kg}^{-1}) = C_{\text{U}} + 1.43 C_{\text{Th}} + 0.077 C_{\text{K}} \quad (4)$$

C_{U} , C_{Th} and C_{K} are the specific activities of ^{238}U , ^{232}Th and ^{40}K in Bq kg^{-1} , respectively.

External hazard index (H_{ex})

External hazard index is used to measure external damage due to emitted gamma radiation and this value is calculated by Eq. 5 [22].

$$H_{\text{ex}} = C_{\text{U}}/370 + C_{\text{Th}}/259 + C_{\text{K}}/4810 \quad (5)$$

C_{U} , C_{Th} and C_{K} are the specific activities of ^{238}U , ^{232}Th , and ^{40}K in Bq kg^{-1} , respectively. For radiation damage to be negligible, the value of H_{ex} must be less than 1.

Absorbed gamma dose rate (D)

The gamma dose rate absorbed in the air 1 m above the surface is obtained by multiplying the specific activity concentrations with certain conversion factors and its formula is given in Eq. 6 [23].

$$D(\text{nGy h}^{-1}) = 0.462 C_U + 0.621 C_{Th} + 0.0417 C_K \quad (6)$$

C_U , C_{Th} and C_K are the specific activities of ^{238}U , ^{232}Th and ^{40}K in Bq kg^{-1} , respectively.

Annual effective dose equivalent (AEDE)

The radiation doses that people have been exposed to for 1 year are determined by calculating the annual effective dose equivalents. The ratio of effective dose equivalent to absorbed dose in the air is defined as 0.7 Sv Gy^{-1} for ambient gamma rays converted to intermediate energies. While making these calculations, it is important how long people are exposed to these rays. The exposure factor measures how much time is spent outside the home and is taken as 20%. The annual effective dose equivalent is calculated by Eq. 7 [23].

$$\text{AEDE}(\text{mSv y}^{-1}) = D(\text{nGy h}^{-1}) \times 8760 \text{ h} \times 0.2 \times 0.7 \text{ Sv Gy}^{-1} \times 10^{-6} \quad (7)$$

Lifetime cancer risk (LCR)

Depending on the exposure of an individual to radiation during his lifetime, the probability of developing cancer arises, and this probability is defined by the lifetime cancer risk. The lifetime cancer risk value is calculated by Eq. 8 [24]

$$\text{LCR} = \text{AEDE} \times \text{DL} \times \text{RF} \quad (8)$$

where DL is the average life duration (78 years) and RF is a risk factor. For stochastic effects, the RF value is taken as 0.05 [24]. The world average value of LCR is given as 0.29×10^{-3} [23].

Geostatistics

Geostatistics is a spatial analysis method that takes into account the relationship between samples and the coordinates from which the samples are taken [5]. In this respect, it differs from traditional statistical methods. This method is based on the theory of stationary randomness [25]. In this calculation method, an estimate of the distribution can be calculated over the mean value [26]. In geostatistical calculations, relationships depending on the distances between spatial variables are determined by the semi-variogram function. This function is expressed as the variance of the

difference between two variables at a distance h from each other, as shown in Eq. 9.

$$\gamma(h) = \frac{1}{2N(h)} \sum_{i=1}^{N(h)} (Z(x_i) - Z(x_i + h))^2 \quad (9)$$

h is the Distance between spatial variables, $N(h)$ is the number of h vectors in the study area, $Z(x_i)$ is the the measured value of the spatial variable at point i -th, $Z(x_i + h)$ is the value measured in the $(x_i + h)$ point of the spatial variable. Semi-variogram is a measure of spatial correlation and shows that the amount of similarity will decrease depending on the increase in the distance between two points [27]. The experimental semi-variogram is calculated according to the distances measured in the study area. The theoretical semi-variogram is determined by fitting the experimental semi-variogram with an appropriate parametric function. In this study, the Ordinary Kriging (OK) method, a geostatistical method that is easy to calculate and can predict the distribution at an appropriate mean value, was used [28]. This method is mathematically defined as the best known linear unbiased estimator (BLUE) [29]. The spatial point whose value is to be estimated using the OK method is estimated with the help of the parametric function obtained from the

theoretical semi-variogram, with a weight factor that will ensure that it is more affected by the distance from the close points and less than the far point [30]. The OK method is quite similar to the weighted-average method in the traditional statistical approach. The general equation of the Kriging approach is presented in Eq. 10.

$$Z(x_0) = \sum_{i=1}^N w_i Z(x_i) \quad (10)$$

$Z(x_0)$ is the unknown but predicted Z value at x_0 point, w_i is the weight coefficient used in the estimation of (x_0) and has different values for each $Z(x_i)$, $Z(x_i)$ is the experimental measurement value used to estimate $Z(x_0)$ and N is the number of spatial data used in the estimation of $Z(x_0)$. In the last decade years, geostatistical methods have been used in many studies to map natural or artificial radioactivity and to estimate the activity values of intermediate points whose measurement value is unknown [5, 29, 31–36].

Table 1 The concentrations of ^{238}U , ^{232}Th , ^{137}Cs and ^{40}K in Şavşat Black Lake sediment samples

Sam- ple code	Activity concentration (Bq kg ⁻¹)			
	^{238}U	^{232}Th	^{137}Cs	^{40}K
SKS-1	18.12 ± 0.93	18.79 ± 1.07	0.86 ± 0.14	551.38 ± 11.28
SKS-2	11.03 ± 0.81	11.62 ± 1.80	101.62 ± 2.53	479.73 ± 23.69
SKS-3	10.30 ± 0.77	10.16 ± 1.25	103.67 ± 1.63	185.88 ± 8.13
SKS-4	8.32 ± 0.91	6.65 ± 0.55	40.69 ± 1.63	379.64 ± 18.57
SKS-5	18.60 ± 1.73	20.20 ± 1.48	215.76 ± 2.77	401.60 ± 15.45
SKS-6	8.19 ± 0.88	5.83 ± 0.68	206.87 ± 3.95	288.10 ± 18.18
SKS-7	27.75 ± 2.60	23.96 ± 2.67	290.82 ± 4.93	471.34 ± 24.05
SKS-8	12.76 ± 0.61	11.77 ± 0.83	1.62 ± 0.30	501.04 ± 10.71
SKS-9	11.08 ± 0.89	11.90 ± 0.97	52.33 ± 1.55	478.02 ± 17.49
SKS-10	17.88 ± 1.40	16.44 ± 1.77	204.92 ± 3.35	419.46 ± 17.83
SKS-11	32.67 ± 2.72	33.08 ± 3.29	438.04 ± 6.89	589.30 ± 30.46
SKS-12	8.15 ± 0.54	15.71 ± 1.51	67.49 ± 1.49	441.29 ± 13.88
SKS-13	13.47 ± 1.14	12.86 ± 1.81	34.65 ± 1.66	432.58 ± 17.14
SKS-14	14.32 ± 1.41	13.35 ± 1.21	175.93 ± 3.77	365.79 ± 19.43
SKS-15	19.86 ± 1.17	18.13 ± 1.16	13.94 ± 0.70	581.52 ± 13.71
SKS-16	10.58 ± 0.64	10.80 ± 0.94	1.87 ± 0.20	480.39 ± 12.03
SKS-17	9.04 ± 0.54	7.00 ± 0.58	143.81 ± 2.71	472.92 ± 11.99
SKS-18	22.79 ± 2.41	17.97 ± 2.11	71.87 ± 2.48	415.42 ± 21.63
SKS-19	11.60 ± 0.63	12.26 ± 0.85	1.46 ± 0.55	473.32 ± 11.71

Results and discussion

Specific activities

Minimum detectable activity (MDA) values for the germanium detector used in the study for ^{238}U , ^{232}Th and ^{40}K radioisotopes were calculated as 0.24 Bq kg⁻¹, 0.21 Bq kg⁻¹ and 2.49 Bq kg⁻¹, respectively. The activity concentrations values found for the radioisotopes ^{238}U , ^{232}Th , ^{137}Cs and ^{40}K in the sediment samples taken from Şavşat Black Lake are given in Table 1. In the sediment samples, the activity concentrations of ^{238}U , ^{232}Th , ^{137}Cs and ^{40}K varied from 8.15 to 32.67, 5.83 to 33.08, 0.86 to 438.04 and 185.88 to 589.30 Bq kg⁻¹, respectively and their mean values are 15.08 ± 1.20 , 14.66 ± 1.40 , 114.12 ± 2.28 and 442.56 ± 16.70 Bq kg⁻¹. World averages for ^{238}U , ^{232}Th and ^{40}K radioisotopes in sediments are given as 35, 30 and 400 Bq kg⁻¹ by UNSCEAR, respectively [23]. The average activity concentrations of ^{238}U and ^{232}Th determined in the

sediment samples taken from Black Lake were lower than the world average, but the average activity concentration of ^{40}K was higher than the world average. The detection of the ^{137}Cs radioisotope in the sediment samples of the lake shows that the effects of the reactor accident that occurred in the Chernobyl Nuclear Power Plant, which is close to studied region and Turkey, as well as the effects of the nuclear tests, still continue, albeit to a small extent.

The distribution and statistical summaries of the radioactivity concentrations determined in the sediment samples taken from Black Lake are shown graphically in Fig. 3. The box graph in the middle of these graphs presents statistical summaries of the data, while the curves on the sides show the scattering density of the data (in which range is the data frequency).

Diagrams of cross-validation and error distributions of interpolation maps created for sediment samples taken from Black Lake are shown in Fig. 4. In the cross-validation process, one observation point is excluded from the data set and this point is estimated through the Kriging model created using other points. This process is repeated for all data in the study. At the end of the calculation, the predicted values of the model versus the actual measurement data are shown with a diagram. Confidence levels of the predicted values (95% and 68%) were determined by the probability curve. In addition, the standard errors between the forecast and the actual values were calculated, and the distribution graph of the standard errors was created. The standard error distribution is expected to be normal to create an appropriate distribution map. The study determined that the error distributions of the distribution maps and Kriging estimates obtained for each radionuclide were normal. As seen in Fig. 3, it can be said that the ^{238}U , ^{232}Th , ^{40}K and ^{137}Cs activity concentrations in the sediment samples generally show a homogeneous distribution. The interpolation maps created for the sediment samples taken from Şavşat Black Lake are given in Fig. 5. These interpolation maps reveal the general pattern of radionuclide activity distributions and show estimate of an average activity concentration for unmeasured areas. According to these maps, it is observed that both natural and artificial radionuclide activity is at high levels, especially in the middle and inner parts of the lake, while the concentration of radiation activity towards the shores generally decreases. The main reason for this is thought to be originate from the increase of sediment accumulation due to the deepening in the middle part of the lake.

The comparison of the average activity concentration values of the ^{238}U , ^{232}Th , ^{40}K and ^{137}Cs radioisotopes determined in the sediment samples of Şavşat Black Lake with the values reported in other studies in the literature is given in Table 2.

As shown in Table 2, the ^{238}U and ^{232}Th concentrations determined in the sediment samples in this study are close

Fig. 3 Activity concentrations and distributions of the Şavşat Black Lake sediment samples

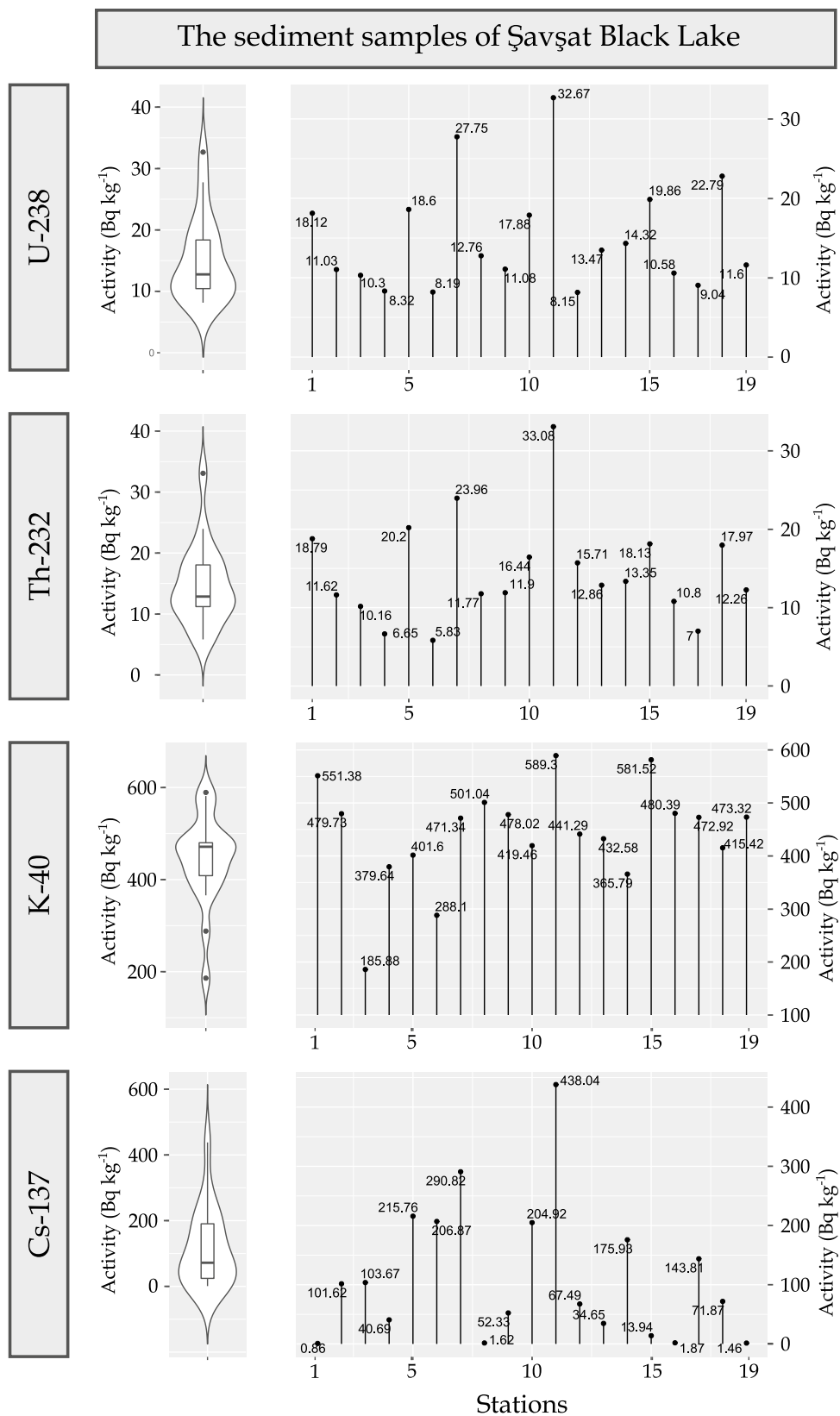
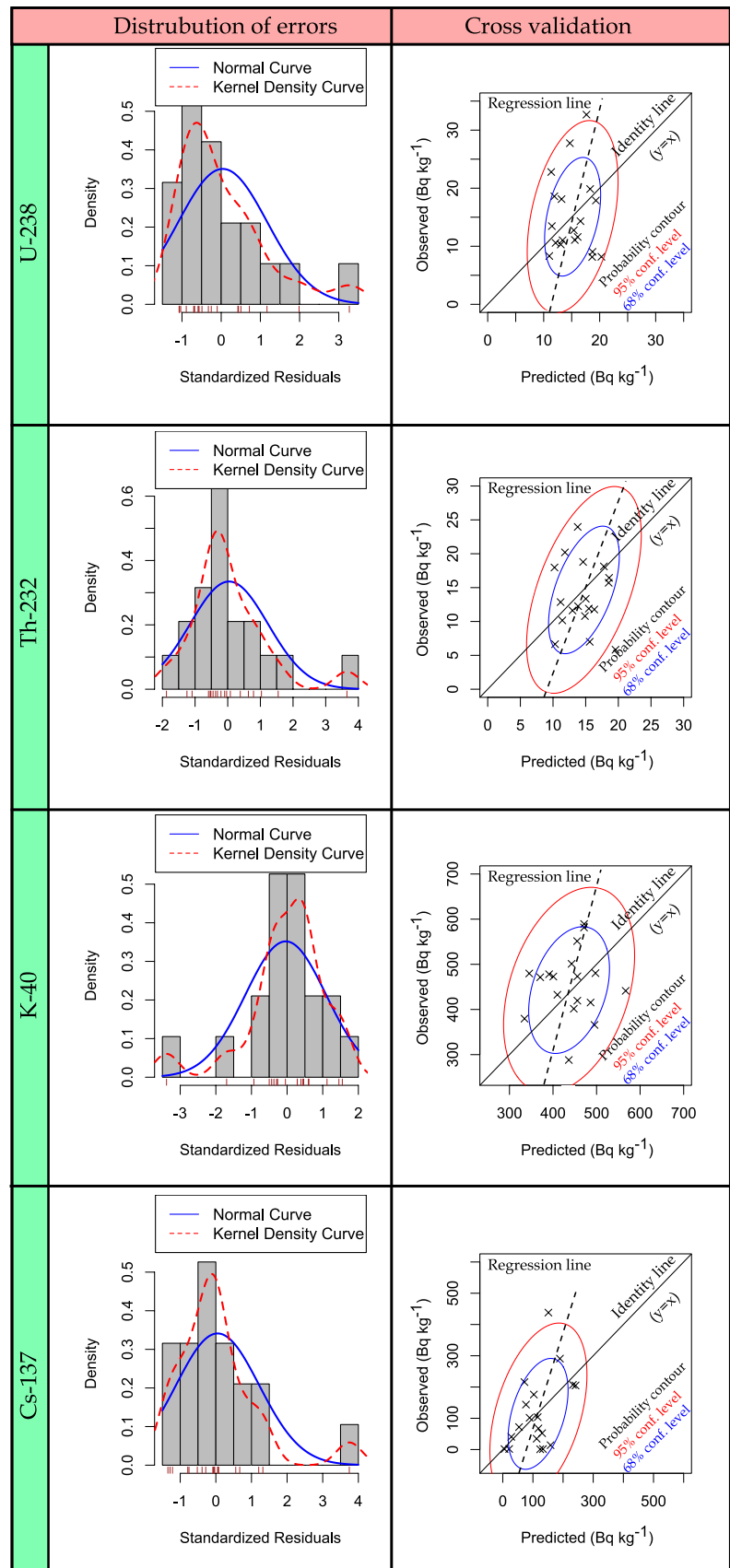


Fig. 4 Cross-validation diagrams of Ordinary Kriging interpolated estimation for the Şavşat Black Lake sediment samples



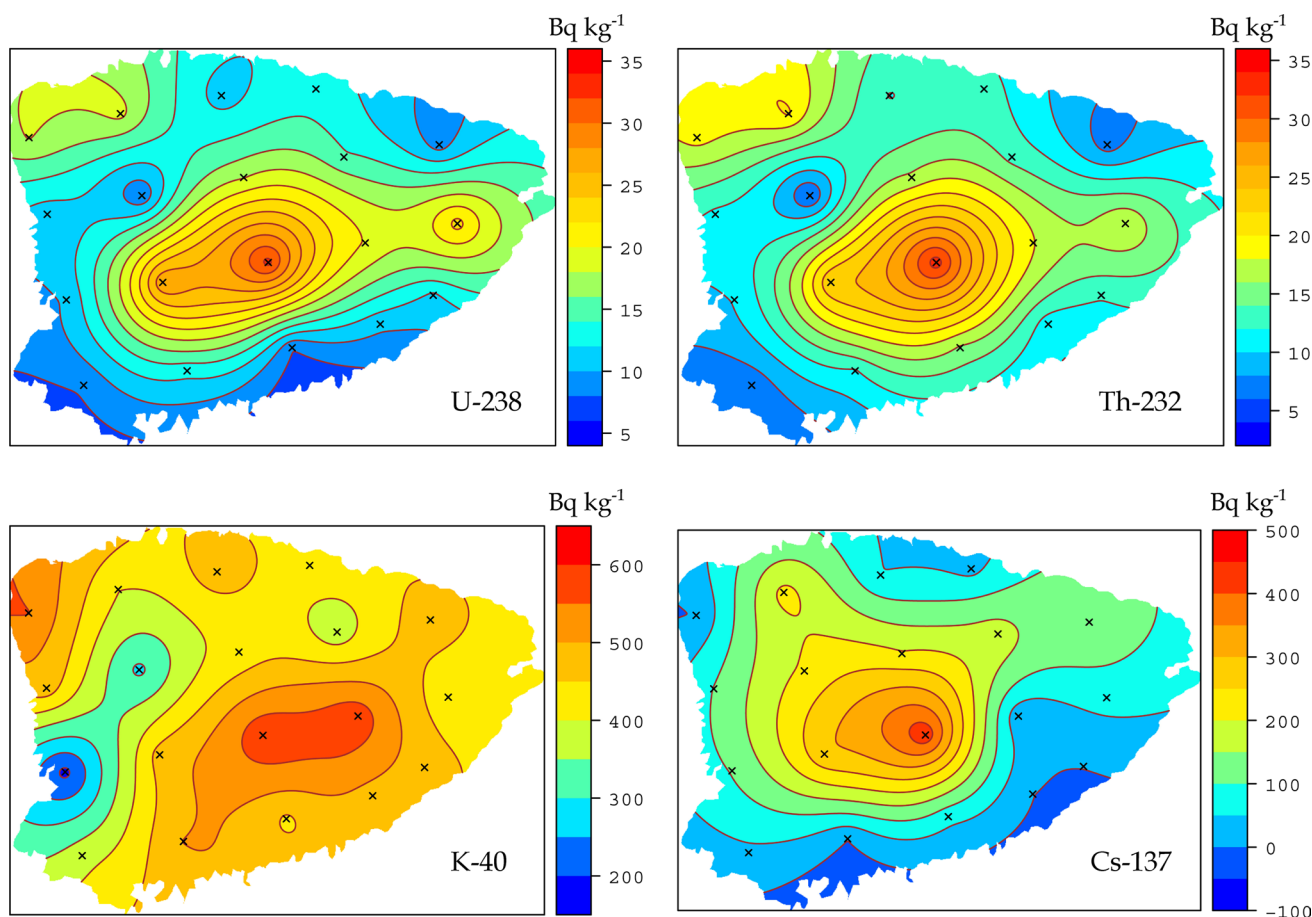


Fig. 5 Geo-spatial distribution maps of the activity concentrations of ^{238}U , ^{232}Th , ^{40}K and ^{137}Cs for the Şavşat Black Lake sediment samples

Table 2 Comparison of activity concentrations determined in the sediment samples with some studies in the literature

Country, lake	Activity concentration (Bq kg ⁻¹)				References
	^{238}U	^{232}Th	^{40}K	^{137}Cs	
Egypt, Brullus	12.3	15.7	227.0	3.7	[37]
Nigeria, Oguta	47.89	55.37	1023	–	[38]
Kenya, Nakuru	36.9	43.5	708.3	–	[39]
Egypt, Tamsah	8.64	13.77	141.6	–	[40]
Egypt, Nasser	14.3	18.4	317.6	2.3	[41]
Turkey, Van	41.61	45.26	713.16	7.61	[42]
Turkey, Eğirdir	34.13	27.32	363.28	–	[43]
Turkey, Şavşat Black Lake	15.08	14.66	442.56	114.12	This study

to the concentrations found in Brullus, Tamsah and Nasser lakes, but lower than the concentrations found in Oguta, Nakuru, Van and Eğirdir lakes. Again, the ^{40}K concentrations determined in the studied sediment samples are higher than the concentrations found in Brullus, Tamsah, Nasser

and Eğirdir lakes, but lower than the concentrations found in Oguta, Nakuru and Van lakes. The ^{137}Cs radioisotope concentrations determined in the sediment samples in this study were found to be considerably higher than the ^{137}Cs concentrations found in all lakes, as can be seen from the table. The fact that ^{137}Cs concentrations are so high compared to other lakes indicates that the region where the lakes are located has highly been contaminated due to the Chernobyl Nuclear Power Plant accident and its effect still continues [15, 44].

Evaluation of radiological hazards

In order to evaluate the radiological hazards originating from the radioisotopes determined in the examined sediment samples, radium equivalent activity (R_{eq}), external hazard index (H_{ex}), absorbed gamma dose rate (D), annual effective dose equivalent (AEDE) and lifetime cancer risk (LCR) values were calculated. These calculated values are given in Table 3.

As can be seen from Table 3, radium equivalent activities (R_{eq}) originating from natural radioactivity of the

Table 3 Radiological hazard parameters calculated in Şavşat Black Lake sediment samples

Sample code	Ra _{eq} (Bq kg ⁻¹)	H _{ex}	D (nGy h ⁻¹)	AEDE (µSv y ⁻¹)	LCR (× 10 ⁻⁵)
SKS-1	87.45	0.24	43.89	53.82	18.84
SKS-2	64.59	0.17	33.03	40.51	14.18
SKS-3	39.14	0.11	19.12	23.44	8.21
SKS-4	47.06	0.13	24.28	29.78	10.42
SKS-5	78.41	0.21	38.58	47.32	16.56
SKS-6	38.71	0.10	19.74	24.22	8.48
SKS-7	98.31	0.27	47.98	58.84	20.59
SKS-8	68.17	0.18	34.78	42.66	14.93
SKS-9	64.90	0.18	33.16	40.67	14.24
SKS-10	73.69	0.20	36.55	44.83	15.69
SKS-11	125.35	0.34	61.19	75.04	26.26
SKS-12	64.59	0.17	32.86	40.29	14.10
SKS-13	65.17	0.18	32.87	40.31	14.11
SKS-14	61.58	0.17	30.68	37.63	13.17
SKS-15	90.56	0.24	45.49	55.79	19.53
SKS-16	63.01	0.17	32.32	39.64	13.87
SKS-17	55.46	0.15	28.83	35.36	12.37
SKS-18	80.47	0.22	39.49	48.43	16.95
SKS-19	65.58	0.18	33.42	40.99	14.35

sediment samples taken from Black Lake varied between 38.71 and 125.35 Bq kg⁻¹ and its average value was found to be 70.12 Bq kg⁻¹. The radium equivalent activities found for sediment samples were below the world average of 370 Bq kg⁻¹ recommended by UNSCEAR [23].

The external hazard indexes (H_{ex}) calculated for the sediment samples taken from Black Lake ranged from 0.10 to 0.34 (Table 3) with an average value of 0.19. All external hazard index values found for sediment samples were below the world average (≤ 1) [12].

As shown in the 4th column of Table 3, the absorbed gamma dose rate (D) values were calculated for the sediment samples taken from Black Lake ranging between 19.12 and 61.19 nGy h⁻¹, and the average value was found to be 35.17 nGy h⁻¹. All D values found for the sediment samples were below the world average of 84 nGy h⁻¹ [12].

The annual effective dose equivalent (AEDE) values calculated for the sediment samples taken from Black Lake ranged from 23.44 to 75.04 µSv y⁻¹ (Table 3), with an average value of 43.13 µSv y⁻¹. All AEDE values obtained from the calculation were found below the world average (520 µSv y⁻¹) [12].

Lifetime cancer risk (LCR) values calculated for sediment samples taken from Black Lake ranged between 8.21×10^{-5} and 26.26×10^{-5} and the average value was found to be

15.10×10^{-5} . All LCR values given in column 6 of Table 3 were below the world average value of 0.29×10^{-3} [12, 23].

Considering the radiological hazard parameters calculated for sediment samples, it was determined that the values found were lower than the world averages. Therefore, it is possible to state that the examined sediment samples do not pose any risk radiologically.

Conclusion

Determination of background radiation levels is important to assess radiation-related health risks. In this study, the concentrations of ²³⁸U, ²³²Th, ⁴⁰K and ¹³⁷Cs in 19 sediment samples taken from Şavşat Black Lake in the National Park in Artvin province were determined using a High Purity Germanium Detector (HPGe). While the concentrations of ²³⁸U and ²³²Th determined in the sediment samples were found to be lower than the values recommended by UNSCEAR, the concentration of ⁴⁰K was found to be high. In addition, ¹³⁷Cs artificial radioisotope was detected in all sediment samples. This can be attributed to the Chernobyl nuclear power plant accident and atmospheric nuclear weapons tests carried out by several countries. From the concentration values determined in the sediment samples, radium equivalent activity (Ra_{eq}), external hazard index (H_{ex}), absorbed gamma dose rate (D), annual effective dose equivalent (AEDE), and lifetime cancer risk (LCR) values were calculated and compared with the values recommended by international organizations. As a result, it can be said that the radioactivity originating from the examined sediment samples does not pose any risk to human health. Moreover, the results of this study can be used as a reference for future studies. In addition, the results obtained will likely contribute to the environmental radioactivity database.

Acknowledgements We thank the our driver Ahmet As for help during the sampling. We would like to thank graduate student Didem Kart for assistance in analyses of samples.

Funding This study was supported by the Recep Tayyip Erdogan University's Scientific Research Projects Department (Project Code: FBA-2019-1003).

Declarations

Conflict of interest The authors declare that they have no conflict of interest.

Ethical approval Not applicable.

Consent to participate Not applicable.

Consent for publication Not applicable.

References

- Sarı S, Dizman S (2020) Investigation of radioactivity and radiological effects in soil samples taken from Ovit Dağbaşı Lake. *El-Cezeri Journal of Science and Engineering* 2020:1122–1130. <https://doi.org/10.31202/ecjse.735215>
- UNSCEAR (1993) Exposure from natural sources of radiation of radiation. United Nations Scientific Committee on the Effects of Atomic Radiation report to United Nations. UNSCEAR, New York
- Otansev P, Taşkın H, Başsarı A, Varinlioğlu A (2016) Distribution and environmental impacts of heavy metals and radioactivity in sediment and seawater samples of the Marmara Sea. *Chemosphere* 154:266–275. <https://doi.org/10.1016/j.chemosphere.2016.03.122>
- Dizman S, Görür FK, Keser R, Görür O (2019) The assessment of radioactivity and radiological hazards in soils of Bolu province, Turkey. *Environ Forensics* 20:211–218. <https://doi.org/10.1080/15275922.2019.1629129>
- Yeşilkanat CM, Kobya Y, Taşkın H, Çevik U (2015) Dose rate estimates and spatial interpolation maps of outdoor gamma dose rate with geostatistical methods; A case study from Artvin, Turkey. *J Environ Radioact* 150:132–144. <https://doi.org/10.1016/j.jenvrad.2015.08.011>
- Wang J, Du J, Bi Q (2017) Natural radioactivity assessment of surface sediments in the Yangtze Estuary. *Mar Pollut Bull* 114:602–608. <https://doi.org/10.1016/j.marpolbul.2016.09.040>
- Venunathan N, Kaliprasad CS, Narayana Y (2016) Natural radioactivity in sediments and river bank soil of Kallada river of Kerala, South India and associated radiological risk. *Radiat Prot Dosim* 171:271–276. <https://doi.org/10.1093/rpd/ncw073>
- Ramasamy V, Paramasivam K, Suresh G, Jose MT (2014) Function of minerals in the natural radioactivity level of Vaigai River sediments, Tamilnadu, India—spectroscopical approach. *Spectrochim Acta A* 117:340–350. <https://doi.org/10.1016/j.saa.2013.08.022>
- Qureshi AA, Tariq S, Din KU et al (2014) Evaluation of excessive lifetime cancer risk due to natural radioactivity in the rivers sediments of Northern Pakistan. *J Radiat Res Appl Sci* 7:438–447. <https://doi.org/10.1016/j.jrras.2014.07.008>
- Kobya Y, Taşkın H, Yeşilkanat CM et al (2015) Natural and artificial radioactivity assessment of dam lakes sediments in Çoruh River, Turkey. *J Radioanal Nucl Chem* 303:287–295. <https://doi.org/10.1007/s10967-014-3420-7>
- Dizman S, Görür FK, Keser R (2016) Determination of radioactivity levels of soil samples and the excess of lifetime cancer risk in Rize province, Turkey. *Int J Radiat Res* 14:237–244. <https://doi.org/10.18869/acadpub.ijrr.14.3.237>
- Sathish V, Chandrasekaran A, Manigandan S et al (2022) Assessment of natural radiation hazards and function of heat production rate in lake sediments of Puliyanthangal Lake surrounding the Ranipet industrial area, Tamil Nadu. *J Radioanal Nucl Chem* 331:1495–1505. <https://doi.org/10.1007/s10967-022-08207-2>
- Kobya Y, Taşkın H, Yeşilkanat CM, Çevik U (2015) Evaluation of outdoor gamma dose rate and cancer risk in Artvin Province, Turkey. *Hum Ecol Risk Assess* 21:2077–2085. <https://doi.org/10.1080/10807039.2015.1017876>
- Yeşilkanat CM, Kobya Y (2015) Determination and mapping the spatial distribution of radioactivity of natural spring water in the Eastern Black Sea Region by using artificial neural network method. *Environ Monit Assess* 187: 589. <https://doi.org/10.1007/s10661-015-4811-0>
- Topcuoğlu S, Kut D, Esen N et al (2001) ¹³⁷Cs in biota and sediment samples from Turkish coast of the Black Sea, 1997–1998. *J Radioanal Nucl Chem* 250:381–384. <https://doi.org/10.1023/A:1017932604374>
- Akar B, Şahin B (2016) Diversity and ecology of benthic algae in Karagöl Lake, Karagöl-Sahara National Park (Şavşat, Artvin, Turkey). *Turk J Bot* 40:645–661. <https://doi.org/10.3906/bot-1601-19>
- MGM (2017) Observation data of Artvin province Şavşat district climate station. Turkish State Meteorological Service. <https://www.mgm.gov.tr/veridegerlendirme/il-ve-ilceler-istatistik.aspx?k=A&m=ARTVIN>
- Öz M, Adanur H, Fidan MS, Komut O (2019) Recreational use of protected areas found in the Eastern Black Sea Region. *Gümüşhane University Journal of Social Sciences Institute* 10:340–350. <https://dergipark.org.tr/en/download/article-file/841209>
- Grigorescu EL, Sahagia M, Razdolescu AC et al (2002) Standardization of Eu-152. *Appl Radiat Isot* 56:435–439
- Currie LA (1968) Limits for qualitative detection and quantitative determination. Application to radiochemistry. *Anal Chem* 40:586–593. <https://doi.org/10.1021/ac60259a007>
- Beretka J, Mathew P (1985) Natural radioactivity of Australian building materials, industrial wastes and by-products. *Health Phys* 48:87–95
- Krieger R (1981) Radioactivity of construction materials. *Betonw Fert Techn* 47:468–473
- UNSCEAR (2000) Exposures from natural radiation sources. United Nations Scientific Committee on the Effects of Atomic Radiation Sources Annex B:140
- ICRP (1990) Recommendations of the international commission on radiological protection, vol 21. International Commission on Radiological Protection Publication 60
- Matheron G (1963) Principles of geostatistics. *Econ Geol* 58:1246–1266
- Clark I (1979) Practical geostatistics. Elsevier, London
- Diggle P, Riberio PJ (2007) Model-based geostatistics. Springer, London
- Krige D (1960) On the departure of ore value distributions from the lognormal model in South African gold mines. *J S Afr Inst Min Metall* 1:231–244
- Baume O, Skøien JO, Heuvelink GBM et al (2011) A geostatistical approach to data harmonization—application to radioactivity exposure data. *Int J Appl Earth Obs Geoinf* 13:409–419. <https://doi.org/10.1016/j.jag.2010.09.002>
- Webster R, Oliver MA (2001) Geostatistics for environmental scientists. Wiley, Hoboken
- Sanusi MSM, Ramli AT, Gabdo HT et al (2014) Isodose mapping of terrestrial gamma radiation dose rate of Selangor state, Kuala Lumpur and Putrajaya, Malaysia. *J Environ Radioact* 135:67–74. <https://doi.org/10.1016/j.jenvrad.2014.04.004>
- Kucukomeroglu B, Karadeniz A, Damla N et al (2016) Radiological maps in beach sands along some coastal regions of Turkey. *Mar Pollut Bull* 112:255–264. <https://doi.org/10.1016/j.marpolbul.2016.08.007>
- Kobya Y, Taşkın H, Yeşilkanat CM et al (2015) Radioactivity survey and risk assessment study for drinking water in the Artvin Province, Turkey. *Water Air Soil Pollut*. <https://doi.org/10.1007/s11270-015-2344-3>
- Hiemstra PH, Pebesma EJ, Twenhöfel CJW, Heuvelink GBM (2009) Real-time automatic interpolation of ambient gamma dose rates from the Dutch radioactivity monitoring network. *Comput Geosci* 35:1711–1721. <https://doi.org/10.1016/j.cageo.2008.10.011>
- Dowdall M, Gerland S, Lind B (2003) Gamma-emitting natural and anthropogenic radionuclides in the terrestrial environment of Kongsfjord, Svalbard. *Sci Total Environ* 305:229–240. [https://doi.org/10.1016/S0048-9697\(02\)00478-3](https://doi.org/10.1016/S0048-9697(02)00478-3)
- Caro A, Legarda F, Romero L et al (2013) Map on predicted deposition of Cs-137 in Spanish soils from geostatistical analyses. *J*

- Environ Radioact 115:53–59. <https://doi.org/10.1016/j.jenvrad.2012.06.007>
37. Diab HM, Ramadan AB, Monged MHE (2006) Assessment of natural radioactivity and heavy metals in Burullus Lake, Egypt. *Int J Low Radiat* 3:273–283. <https://doi.org/10.1504/IJLR.2006.012002>
 38. Isinkaye MO, Emelue HU (2015) Natural radioactivity measurements and evaluation of radiological hazards in sediment of Oguta Lake, South East Nigeria. *J Radiat Res Appl Sci* 8:459–469. <https://doi.org/10.1016/j.jrras.2015.05.001>
 39. Langat WK, Omar HN, Ambusso WJ (2012) Gamma ray spectrometric analysis of sediment deposits at the shores of Lake Nakuru, Kenya. *J Nat Sci Res* 4:34–40
 40. Fares S (2017) Measurements of natural radioactivity level in black sand and sediment samples of the Tamsah Lake beach in Suez Canal region in Egypt. *J Radiat Res Appl Sci* 10:194–203. <https://doi.org/10.1016/j.jrras.2017.04.007>
 41. Khater AE, Ebaid YY, El-Mongy SA (2005) Distribution pattern of natural radionuclides in Lake Nasser bottom sediments. *Int Congr Ser* 1276:405–406
 42. Kayakökü H, Dođru M (2017) Radioactivity analysis of soil samples taken from the western and northern shores of Lake Van, Turkey. *Appl Radiat Isot* 128:231–236. <https://doi.org/10.1016/j.apradiso.2017.07.019>
 43. Özseven A, Akkurt I, Günođlu K (2020) Determination of some dosimetric parameters in Eđirdir Lake, Isparta, Turkey. *Int J Environ Sci Technol* 17:1503–1510. <https://doi.org/10.1007/s13762-019-02569-z>
 44. Tařkın H, Yeřilkanat CM, Kobya Y, Çevik U (2018) Evaluation and mapping of radionuclides in the terrestrial environment and health hazard due to soil radioactivity in Artvin, Turkey. *Arab J Geosci* 11:729. <https://doi.org/10.1007/s12517-018-4063-8>

Publisher's Note Springer Nature remains neutral with regard to jurisdictional claims in published maps and institutional affiliations.